Artificial Organs

Artificial Organs
34(10):798–806, Wiley Periodicals, Inc.
© 2010, Copyright the Authors
Artificial Organs © 2010, International Center for Artificial Organs and Transplantation and Wiley Periodicals, Inc.

Flow Analysis of Ventricular Assist Device Inflow and Outflow Cannula Positioning Using a Naturally Shaped Ventricle and Aortic Branch

*Marco Laumen, *Tim Kaufmann, *Daniel Timms, *Peter Schlanstein, *Sebastian Jansen, †Shaun Gregory, *Kai Chun Wong, *Thomas Schmitz-Rode, and *Ulrich Steinseifer

**Department of Cardiovascular Engineering, Institute of Applied Medical Engineering, Helmholtz Institute, RWTH Aachen University, Aachen, Germany; and †School of Engineering Systems and Medical Device Domain, Institute of Health and Biomedical Innovation, Queensland University of Technology, Brisbane, Australia*

Abstract: Tip geometry and placement of rotary blood pump inflow and outflow cannulae influence the dynamics of flow within the ventricle and aortic branch. Cannulation, therefore, directly influences the potential for thrombus formation and end-organ perfusion during ventricular assist device (VAD) support or cardiopulmonary bypass (CPB). The purpose of this study was to investigate the effect of various inflow/outflow cannula tip geometries and positions on ventricular and greater vessel flow patterns to evaluate ventricular washout and impact on cerebral perfusion. Transparent models of a dilated cardiomyopathic ventricle and an aortic branch were reconstructed from magnetic resonance imaging data to allow flow measurements using particle image velocimetry (PIV). The contractile function of the failing ventricle was reproduced pneumatically, and supported with a rotary pump. Flow patterns were visualized around VAD inflow cannulae, with various tip geometries placed in three positions in the ventricle. The outflow cannula was placed in the subclavian artery and at several positions in the aorta. Flow patterns were measured using PIV and used to validate an aortic flow computational fluid dynamic study. The PIV technique indicated that locating the inflow tip in the left ventricular outflow tract improved complete ventricular washout while the tip geometry had a smaller influence. However, side holes in the inflow cannula improved washout in all cases. The PIV results confirmed that the positioning and orientation of the outflow cannula in the aortic branch had a high impact on the flow pattern in the vessels, with a negative blood flow in the right carotid artery observed in some cases. Cannula placement within the ventricle had a high influence on chamber washout. The positioning of the outflow cannula directly influences the flow through the greater vessels, and may be responsible for the occasional reduction in cerebral perfusion seen in clinical CPB. **Key Words:** Computational fluid dynamics—Inflow cannula—Particle image velocimetry—Rotary blood pump—Ventricular assist device.

The numbers of ventricular assist device (VAD) support and cardiopulmonary bypass (CPB) procedures are increasing as the incidence of heart disease continues to expand each year (1). While technological advances for mechanical support have resulted in smaller and less traumatic devices (2,3), the focus on the interaction between the device and the cardiovascular system, and in particular the cannulation technique, has received less attention. The cannulae's shape, design, and positioning directly influence the dynamics of flow within the ventricle and aortic branch during CBP and VAD support. Thus, cannulation has a strong impact on performance and ultimate success of these therapeutic strategies. A successful treatment is assessed by adequate perfusion to the vascular system, and therefore unobstructed device inflow and outflow has to be ensured by correct placement of the cannulae. A further consequence of poor placement is the

doi:10.1111/j.1525-1594.2010.01098.x

Received March 2010; revised June 2010.
Address correspondence and reprint requests to Mr. Marco Laumen, Applied Medical Engineering, Helmholtz Institute, RWTH Aachen University, Pauwelsstrasse 20, Aachen 52074, Germany. E-mail: laumen@hia.rwth-aachen.de
Presented in part at the 17th Congress of the International Society for Rotary Blood Pumps held October 1–3, 2009 in Singapore.

potential increase in neurological disorders caused by thromboembolic events or inadequate cerebral perfusion. A number of studies identified that embolism may be caused by manipulation of the aorta by cannulae or clamps (4–6) or the outflow cannula jet stream hitting the inner aortic wall (7–9). Also, the placement of the VAD inflow cannula influences the cerebrovascular adverse event rate (10). In addition to these factors, the incidence of ventricular collapse during VAD support may also be responsible for reduced end-organ perfusion (11,12). Cannulation, therefore, directly influences the potential for thrombus formation and end-organ perfusion during VAD support or CPB.

The VAD inflow cannula is usually inserted into the left ventricle (LV)(13), while the outflow cannula is conventionally anastomosed or inserted into the ascending aorta. However, other techniques include insertion of the cannula into the subclavian artery during CPB (14) or the right subclavian artery during VAD support (15–17).

The purpose of this study was to quantify the flow patterns within individual anatomic models of the aortic branch and the LV under different cannulation approaches, using particle image velocimetry (PIV). More specifically, the effects of various inflow cannula tip geometries and positions were investigated with respect to potential thrombus formation within the ventricle during VAD support. The outflow within the aorta and greater vessels was also evaluated and the level of cerebral perfusion was assessed. The ultimate goal of this study was to produce safe cannulation recommendations to reduce clinical complications during VAD support and CPB.

MATERIALS AND METHODS

Model creation

As PIV is an optical flow measurement technique, transparent models of the aorta and the ventricle were required. Therefore, magnetic resonance imaging data of a healthy patient and of a patient with a dilated ventricle were recorded. The cardiovascular system was extracted in both cases by Mimics software (Materialise Inc., Leuven, Belgium), using Hounsfield units, mathematical and manual corrections. The final ventricle model represented a dilated LV in end systole with an internal volume of 250 mL. The aortic model included the aorta, subclavian, carotid, and vertebral arteries. These models were modified into thin-walled computer aided design (CAD) models using the software 3-matic (Materialise Inc.). They were printed by a rapid prototyper (Eden 350V, Objet Geometries Ltd., Rehovot, Israel) using an acrylic-based photopolymer material. To reduce surface roughness, both models were polished and coated with a thin layer of water-soluble finish. The aortic model was placed in a custom-made clear perspex molding chamber and molded in transparent silicone (RT 601, Wacker Chemie AG, Munich, Germany). The ventricle model was coated with a silicone layer of 2-mm thickness. In a final step, the printed cores were removed out of the silicone. Figure 1 shows the complete manufacturing process.

Test rigs

The model of the aorta and the model of the ventricle were included in separate mock circulation loops.

Aortic test rig

In the aortic model, two different cannulation approaches were investigated: a tubular shaped cannula (EOPA 77 420, 20Fr, Medtronic, Inc., Minneapolis, MN, USA) was inserted into the right subclavian artery of the silicone model and placed 10 mm from the bifurcation to the right vertebral artery. In a second experiment, a Jostra arterial cannula (A20-7105, MAQUET, Inc., Wayne, NJ, USA) cannula, which has a curved tip design, was placed in the ascending aorta, leading the emerging jet flow toward the aortic wall downstream of the left subclavian bifurcation (see Fig. 2). Both experiments were used to validate computational fluid dynamic (CFD) studies. To obtain a CFD model with the same cannula arrangement, the cannulated silicone model was re-scanned in a computer tomograph. Based on these data, a CAD model was generated and used for flow simulations (18).

In both cannulation approaches, a rotary pump (Deltastream DP2, Medos Medizintechnik AG, Stolberg, Germany) perfused the model with a continuous flow of 4.5 L/min of water/glycerol solution (58/42 by mass). The flow through the outgoing aortic vessels was collected in a reservoir and returned to the pump (see Fig. 3 for the subclavian setup). Ultrasonic flow meters (ME-PXL, H11X15, Transonic Systems Inc., Ithaca, NY, USA) measured the flow in each tube. As the cured silicone and the test fluid had similar refractive indices, the optical distortion was limited.

Ventricle test rig

The fabricated silicone ventricle was suspended in a water/glycerol (58/42 by mass)-filled pressure chamber which was connected to a Medos VAD Drive System (Medos Medizintechnik AG) (see

شکلها حتماً گذاشته شود

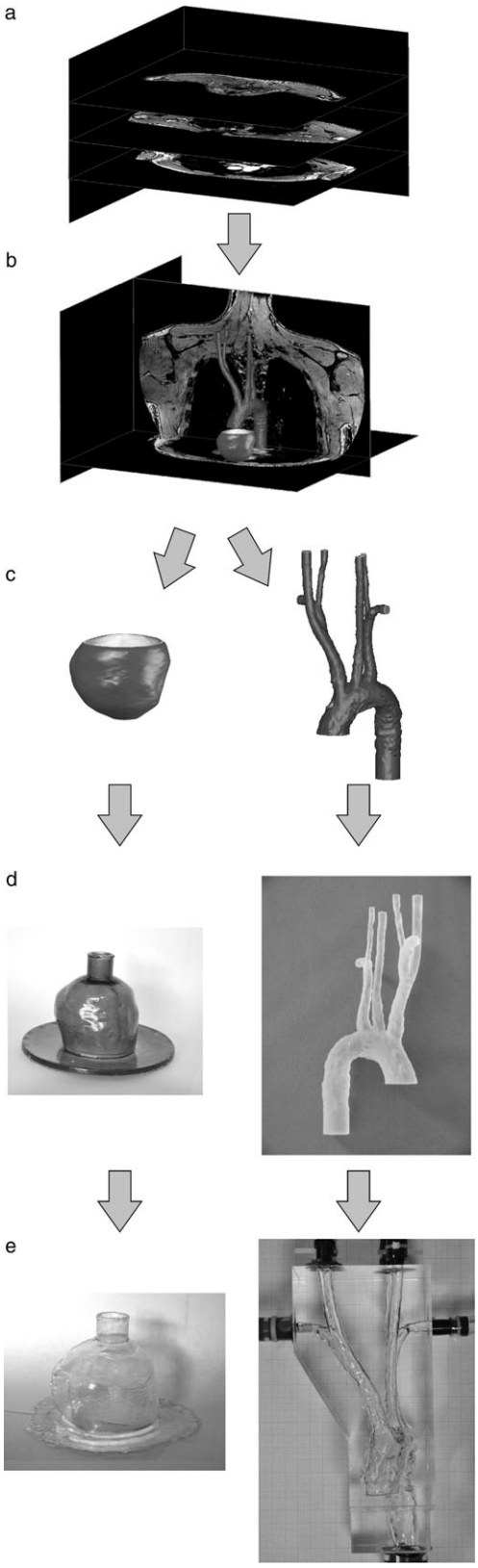

FIG. 1. Model creation: (a) MRI; (b) extracting the cardiovascular system; (c) CAD model; (d) rapid prototyping; and (e) silicone molding.

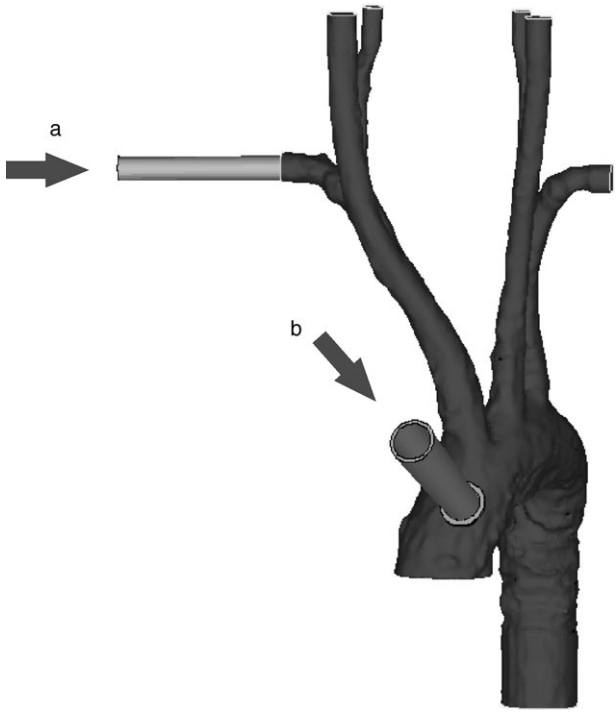

FIG. 2. (a) Cannulation in the right subclavian artery; and (b) cannulation in the ascending aorta.

Fig. 4). By changing the pressure within the pressure chamber, a pulsating ventricle was reproduced.

The ventricle itself was connected to a mock circulation loop to simulate physiological flow conditions. Preload was provided by a hydrostatic head within an atrium chamber. A compliance chamber downstream

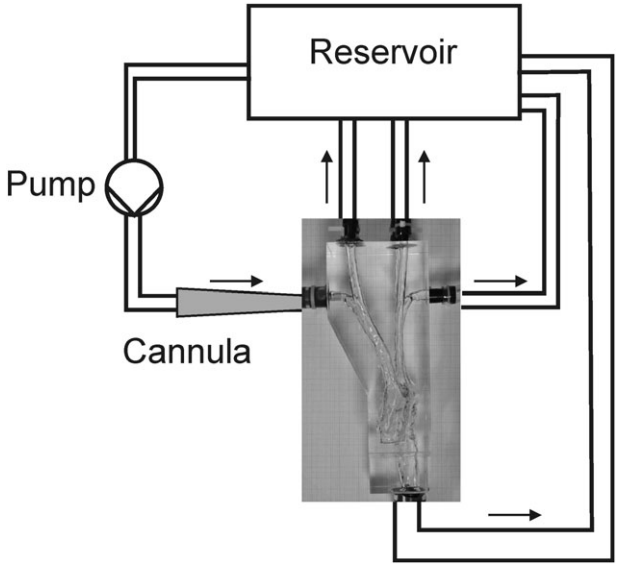

FIG. 3. Aortic test rig with cannulation in the right subclavian artery.

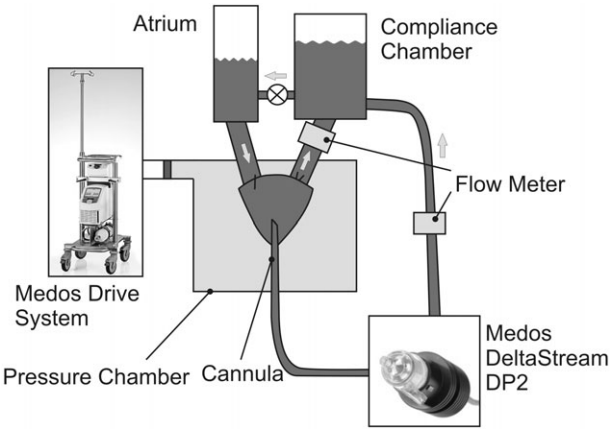

FIG. 4. Ventricular test rig.

of the ventricle simulated the systemic compliance. A throttle between the compliance chamber and atrium was used to adjust the afterload. Mechanical heart valves directed the flow: a Bjork Shiley tilting disc valve was used as the inlet valve and a Carbomedics bi-leaflet valve (Carbomedics, Inc., Austin, TX, USA) acted as the outlet valve. The opening of the inlet valve was considered to direct fluid alongside the LV free wall toward the apex, mimicking the natural inlet blood flow through the mitral valve.

Through the apex of the ventricle, two different cannulae were inserted: an Abiomed Ventricular/Atrial cannula (42Fr., 0506-0142M-VA, ABIOMED Inc., Danvers, MA, USA) with an angular tip design including side holes, and a Ventracor cannula with a trumpet-shaped tip design (Ventracor Ltd., Sydney, Australia). The depth of immersion and orientation were adjustable. Each cannula was connected to a rotary blood pump (Deltastream DP2, Medos Medizintechnik AG), which pumped the fluid from the ventricle into the systemic compliance chamber. The pump could provide steady flow or pulsating flow by changing the rotational speed.

The working fluid was a water/glycerol mixture (58/42 by mass) with a viscosity of 3.6 mPas at room temperature. As the pressure chamber was also filled with this fluid and the thin silicone ventricle had a similar refractive index, optical distortion was limited. The pressure chamber was octagonal with planar side panel sections, thus allowing stereoscopic PIV measurements. Pressures within the mock ventricle, atrium, and aorta were measured with clinical grade pressure sensors (DPT-6000, Codan pvb Critical Care GmbH, Lensahn, Germany) connected to a pressure meter. Aortic flow and pump outlet flow were measured with ultrasound flow probes (ME-PXL, H11X15, Transonic Systems Inc.).

The beating mock ventricle could be synchronized to a pulsation of the blood pump, by using a triggering function created in LabVIEW (National Instruments Corporation, Austin, TX, USA).

PIV

In this study, the flow field was measured with PIV, which is a noninvasive, optical measurement technique. It is based on the movement-detection of illuminated particles within the flow and allows the calculation of a velocity vector map. The technique is described in detail by Raffel et al. (19), while the theoretical background is explained by Keane and Adrian (20,21).

The test fluid was seeded with fluorescent particles with a diameter of 10 µm (Intelligent Laser Applications GmbH, Juelich, Germany). A Nd:YLF Laser (Pegasus, New Wave Research Inc., Fremont, CA, USA) and cylindrical lenses were used to generate a light sheet and illuminate the particles. A 1280 × 1024 CMOS high-speed camera (Nanosense MKIII, Dantec Dynamics A/S, Skovlunde, Denmark) with a 60-mm micro lens (AF Micro-Nikkor 60/F2.8D, Nikon Inc., Melville, NY, USA) captured up to 2000 images per second of the illuminated particles. The camera was equipped with a filter corresponding to the wave of fluorescence so that only the fluorescent light is recorded. Both light sheet optic and camera were mounted to a traverse system (isel AG, Eichenzell, Germany) and moved stepwise to capture the complete measurement volume.

The recorded images were analyzed with adaptive correlation algorithms (Dynamic Studio, Dantec Dynamics). The initial interrogation area (IA) was 64 × 64 pixels, the final IA was 32 × 32 pixels, with an overlap of 25%. Incorrect vectors were eliminated by a moving average validation with an acceptance factor of 0.1. The time between the laser pulses was chosen depending on the fluid velocity to obtain a particle movement of about one-fourth of the IA.

RESULTS

Outflow cannulation in the right subclavian artery

By traversing laser optics and camera, the flow in the complete aortic model was measured under steady-state flow conditions. Figure 5 shows a detailed velocity vector map close to the cannula tip in the right subclavian artery, whereas Fig. 6 depicts the overall flow field in the complete PIV model.

The narrow cannula tip generated a jet flow with high velocities. When this jet passes the diverging vessels, it can function as a suction pump leading to a negative flow in the right carotid artery. This phenom-

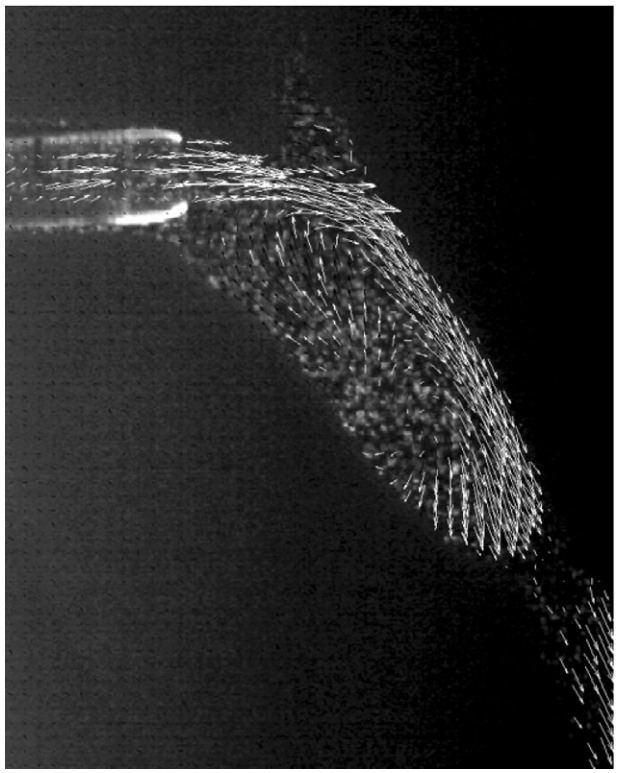

FIG. 5. Velocity vector map close to the cannula tip.

enon is based on the Venturi effect: Due to the increasing velocity, the static pressure decreases. If it falls below the pressure in the collecting reservoir, a negative flow occurs. This effect was very sensitive to the angle and placement of the cannula. The PIV data was used to validate a CFD study, matching the CFD results within 10% accuracy (22). In this CFD study, further cannula positions were investigated.

The used fluid had Newtonian characteristics, whereas blood is a non-Newtonian fluid. To investigate the impact of non-Newtonian fluid characteristics on flow distribution, the experiment was repeated with porcine blood. Table 1 shows the flow through the outgoing vessels for water/glycerol and heparinized porcine blood. In both cases, the flow through the outgoing vessels is similar (see Table 1). In the water/glycerol experiment, total negative number does not equal total positive number due to the measuring inaccuracy of the Transonic flow probes.

Outflow cannulation in the ascending aorta

The cerebral perfusion was again measured during cannulation and the velocity vector maps were measured in different planes within the aortic model. Figure 7 depicts the measured vector field in the central plane of the left subclavian artery. The cannula outflow jet (yellow arrow) splits at the aortic wall. In the left subclavian artery, a vortex pair is observed, while in the left carotid artery, a negative flow into the aortic arch occurs due to the Venturi effect.

Inflow cannulation in the ventricle

During inflow cannulation, the flow was measured in the complete ventricle by traversing the light sheet stepwise through the measurement volume. In the following figures, only an extract of the velocity data is shown. The illustrated planes are very close to the cannula, but the light sheet does not cross the cannula to avoid shadow. Figure 8 gives a top view of the ventricle with the light sheet. Figure 9 depicts the instantaneous velocity vector maps in this plane in end diastole while the Abiomed Cannula was placed close to the apex (Fig. 9a), in the central position (Fig. 9b), in a high (cranial) position (Fig. 9c), and bent toward the outflow tract (Fig. 9d). Every second vector is shown and the contour plot displays the absolute velocity. Due to the moving average validation, less than 3% of the total vectors were interpolated. Total ventricular support was replicated, thus the complete flow was obtained by the pump with a steady flow of 4.5 L/min through the cannula, while the simulated failing ventricle was pulsating at 60 beats per minute.

In all cases, a vortex developed within the ventricle. If the cannula was placed close to the apex (Fig. 9a), this vortex was least distinctive, as the inflow jet entering the ventricle from the mitral valve was for the most part directly sucked into the cannula. Placing the cannula in the center of the ventricle (Fig. 9b), in a high cranial position (Fig. 9c) and bent toward the outflow tract (Fig. 9d), leads to more distinctive vortices within the ventricle. In the last case, high velocity was maintained alongside a larger segment of the ventricular wall, which appears to result in a greater degree of apical and left ventricular outflow tract (LVOT) washout compared with the other cannulae placements.

Similar measurements were repeated with the trumpet-shaped Ventracor cannula. In general, the results were similar, although the vortex center was less focused around the cannula tip due to the lack of side holes. This is illustrated in Fig. 10 where averaged velocity maps over two cycles (1000 images averaged) are shown. In that way, these velocity maps are not instantaneous but demonstrate the main flow characteristics for a conventionally placed cannula in the center of the ventricle.

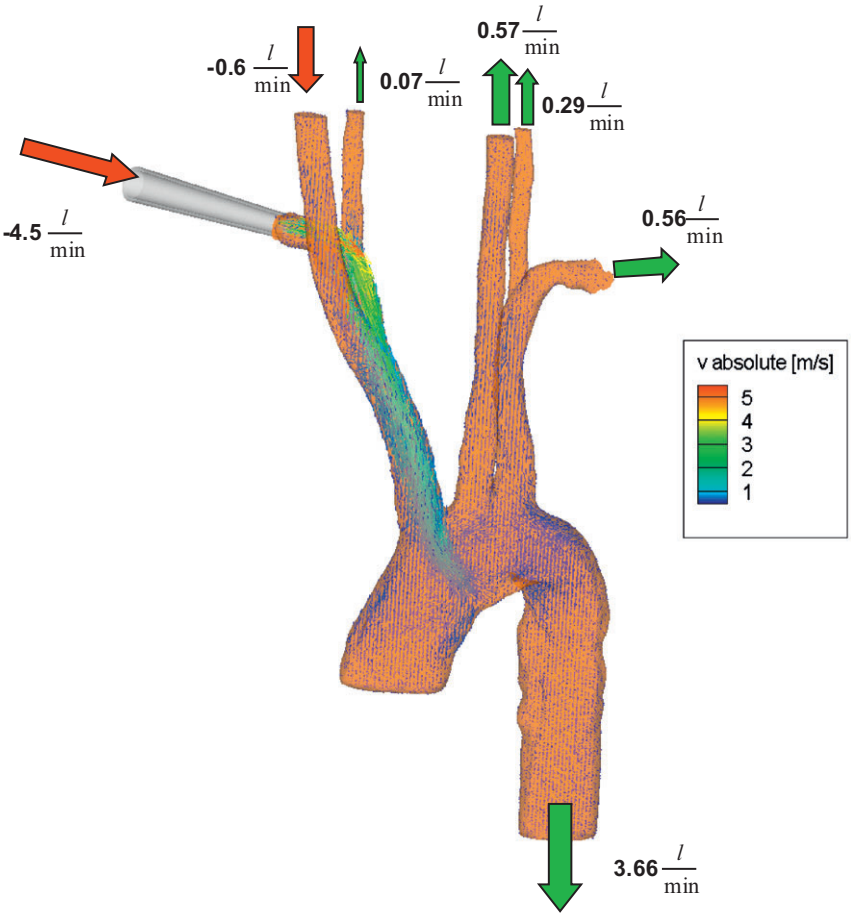

FIG. 6. Flow distribution in the complete model.

DISCUSSION

Both placement of the inflow and outflow cannula had a high impact on the respective blood flow through the ventricular chamber and greater vessels. The placement of the outflow cannula in the aortic model could lead to a negative flow in the cerebral vessels. This occurred due to the Venturi effect if the cannula in the right subclavian artery was placed close to the vertebral branch, or if the outflow jet of

TABLE 1. *Flow through the model*

	Water/glycerol	Porcine blood
Cannula	–4.45	–4.5
Right vertebral artery	0.07	0.08
Right carotid artery	–0.6	–0.2
Left carotid artery	0.57	0.43
Left vertebral artery	0.29	0.2
Left subclavian	0.56	0.5
Aorta	3.66	(3.7)

A negative value indicates a flow into the model; a positive value indicates a flow out of the model.

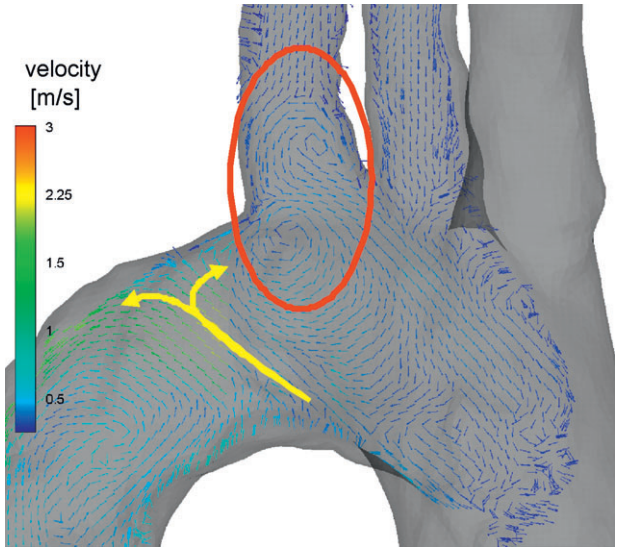

FIG. 7. Velocity vector map during cannulation in the ascending aorta.

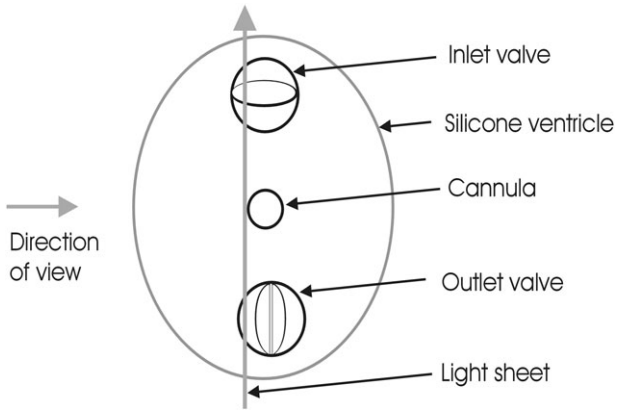

FIG. 8. Top view of the ventricle with the cutting light sheet.

the cannula in the ascending aorta was directed alongside the arteria subclavia sinistra. Correct placement of the cannulae seems to be crucial during CBP and VAD support. However, in our aortic model, cerebral autoregulation and the individual vessel resistance were not applied. Cerebral autoregulation is the intrinsic ability to maintain sufficient blood flow despite changes in perfusion pressure (23). Thus, the observed phenomena may differ from a patient's blood flow. Nevertheless, these in vitro measurements could be used to recommend cannulation techniques, as the model represents a "worst case scenario" without any autoregulation.

During ventricular cannulation, we assume that a large vortex with high velocities along the ventricular walls would increase the washout. An improved washout could reduce the potential for thrombus

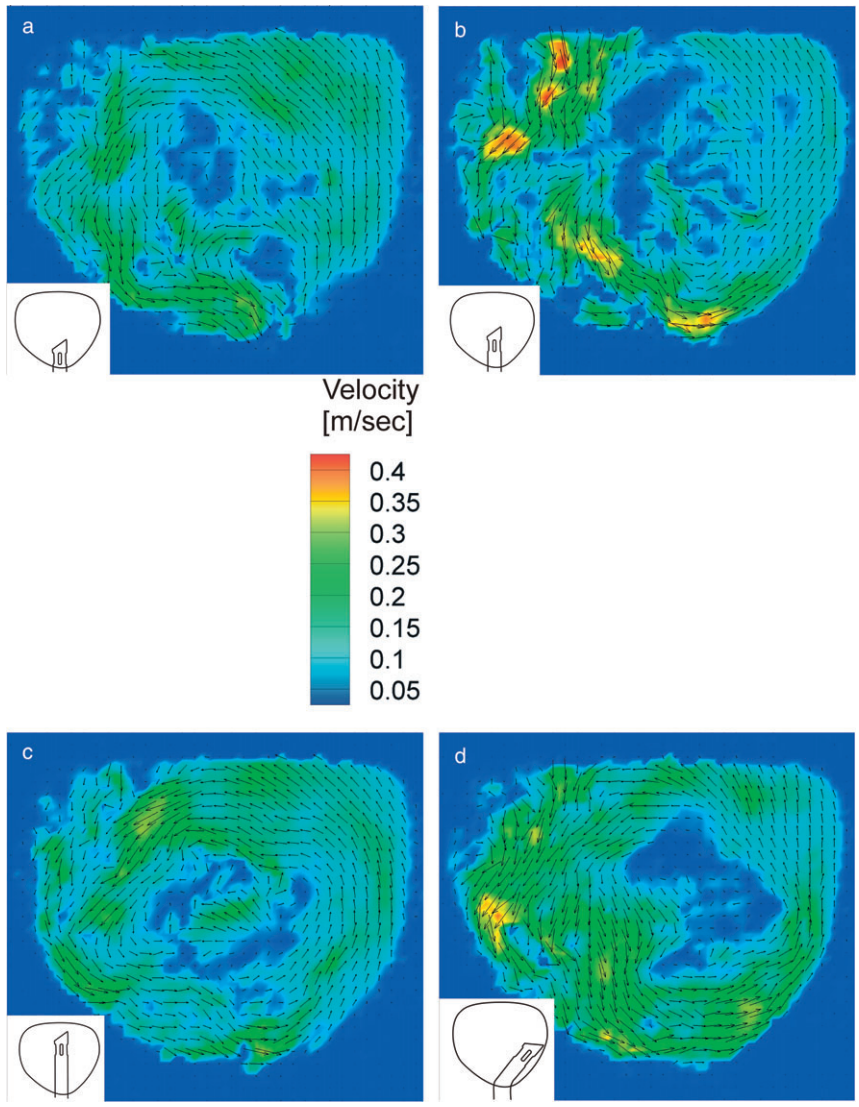

FIG. 9. Velocity vector maps (a) cannula close to the apex; (b) in the central position; (c) in a high (cranial) position; and (d) bent toward the outflow tract.

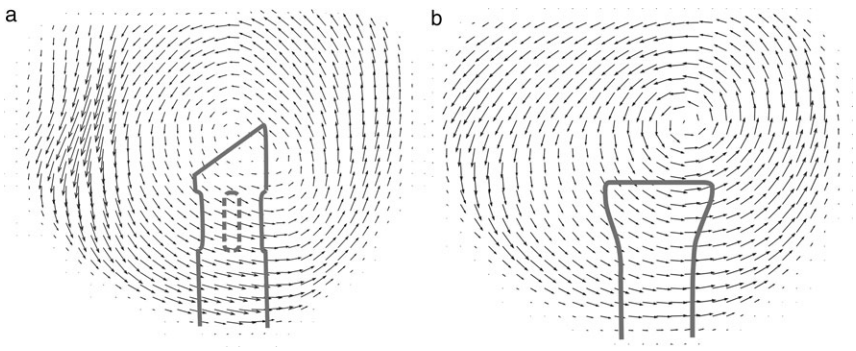

FIG. 10. Cannula placement in the center of the ventricle: (a) Abiomed cannula; and (b) Ventracor cannula.

formation. Under this aspect, placement of the cannula bent toward the LVOT would lead to the most distinctive vortices. Furthermore, a placement in the outflow tract allows the inflow jet during diastole to propagate with high velocities to the apex. This could lead to good washout around the cannula insertion point. The tip design (square/angled) had smaller influence, but side holes created more distinctive vortex centers around the cannula tip.

For our measurements, a mixture of water and glycerol was used as test fluid with Newtonian fluid characteristics, whereas blood is a non-Newtonian fluid. To estimate the difference, we repeated the aortic experiment with heparinized porcine blood and showed that the absolute flow through the vessels was similar. It has to be taken into account that the heparinization affects the blood rheology (24).

The silicone model of the ventricle was fabricated in end-systolic shape. In this way, pulsation could be obtained by extending the ventricular volume. When the VAD was switched on, this volume was reduced, leading to a folding of the silicone wall. This could influence the flow in an unphysiological way, although it is not clear what happens with a patient's ventricle walls during VAD support.

Because individual human data sets were used for fabrication of both models, the transferability of the results to wider patient's range is limited. Nevertheless, these models are produced with a high anatomic accuracy leading to realistic measurements.

CONCLUSION

Both the aortic and the ventricular test rig proved the feasibility to perform accurate flow measurements using PIV. It was shown that cannula placement has a high impact on blood flow, with a negative blood flow in the right carotid artery observed in some cases. Thus, cannula placement may be responsible for the occasional reduction in cerebral perfusion seen in clinical CPB.

Flow measurements in the ventricle suggested placement of the VAD inflow cannula in the LVOT to improve ventricular chamber washout.

A combination of both test rigs will allow us to get a detailed insight in the flow characteristics of essential parts of the cardiovascular system. At the same time, different VAD running strategies can be tested and the impact on the flow field can be investigated both in the ventricle and the aorta.

REFERENCES

1. Thunberg CA, Gaitan BD, Arabia FA, Cole DJ, Grigore AM. Ventricular assist devices today and tomorrow. *J Cardiothorac Vasc Anesth* 2010;10.1053/j.jvca.2009.11.011.
2. Frazier OH, Myers TJ, Gregoric ID, et al. Initial clinical experience with the jarvik 2000 implantable axial-flow left ventricular assist system. *Circulation* 2002;105:2855–60.
3. Garatti A, Colombo T, Russo C, et al. Impella recover 100 microaxial left ventricular assist device: the niguarda experience. *Transplant Proc* 2004;36:623–6.
4. Nakamura K, Harasaki H, Fukumura F, Fukamachi K, Whalen R. Comparison of pulsatile and non-pulsatile cardiopulmonary bypass on regional renal blood flow in sheep. *Scand Cardiovasc J* 2004;38:59–63.
5. Scarborough JE, White W, Derilus FE, Mathew JP, Newman MF, Landolfo KP. Neurologic outcomes after coronary artery bypass grafting with and without cardiopulmonary bypass. *Semin Thorac Cardiovasc Surg* 2003;15:52–62.
6. Verdonck PR, Siller U, De Wachter DS, De Somer F, Van Nooten G. Hydrodynamical comparison of aortic arch cannulae. *Int J Artif Organs* 1998;21:705–13.
7. Fukae K, Tominaga R, Tokunaga S, Kawachi Y, Imaizumi T, Yasui H. The effects of pulsatile and nonpulsatile systemic perfusion on renal sympathetic nerve activity in anesthetized dogs. *J Thorac Cardiovasc Surg* 1996;111:478–84.
8. Kapetanakis EI, Stamou SC, Dullum MKC, et al. The impact of aortic manipulation on neurologic outcomes after coronary artery bypass surgery: a risk-adjusted study. *Ann Thorac Surg* 2004;78:1564–71.
9. Undar A, Masai T, Frazier OH, Fraser CD. Pulsatile and nonpulsatile flows can be quantified in terms of energy equivalent pressure during cardiopulmonary bypass for direct comparisons. *ASAIO J* 1999;45:610–4.
10. Schmid C, Jurmann M, Birnbaum D, et al. Influence of inflow cannula length in axial-flow pumps on neurologic adverse event rate: results from a multi-center analysis. *J Heart Lung Transplant* 2008;27:253–60.
11. Mason DG, Hilton AK, Salamonsen RF. Reliable suction detection for patients with rotary blood pumps. *ASAIO J* 2008;54:359–66.

12. Voigt O, Benkowski RJ, Morello GF. Suction detection for the micromed debakey left ventricular assist device. *ASAIO J* 2005;51:321–8.
13. Meyns B, Siess T, Nishimura Y, et al. Miniaturized implantable rotary blood pump in atrial-aortic position supports and unloads the failing heart. *Cardiovasc Surg* 1998;6:288–95 CVE.
14. Gerdes A, Joubert-Hübner E, Esders K, Sievers HH. Hydrodynamics of aortic arch vessels during perfusion through the right subclavian artery. *Ann Thorac Surg* 2000;69:1425–30.
15. Meyns B, Dens J, Sergeant P, Herijgers P, Daenen W, Flameng W. Initial experiences with the impella device in patients with cardiogenic shock—impella support for cardiogenic shock. *Thorac Cardiovasc Surg* 2003;51:312–7.
16. Meyns B, Klotz S, Simon A, et al. Proof of concept: hemodynamic response to long-term partial ventricular support with the synergy pocket micro-pump. *J Am Coll Cardiol* 2009;54:79–86.
17. WorldHeart Corporation. Minimally invasive VAD (MiVAD). 2010. Available at: http://www.worldheart.com/technologies/mivad.cfm. Accessed March 1, 2010.
18. Kaufmann TAS, Hormes M, Laumen M, et al. The impact of aortic/subclavian outflow cannulation for cardiopulmonary bypass and cardiac support: a computational fluid dynamics study. *Artif Organs* 2009;33:727–32.
19. Raffel M, Willert CE, Wereley ST, Kompenhans J. *Particle Image Velocimetry—A Practical Guide*, 2nd Edition. Berlin: Springer Verlag, 2007.
20. Adrian RJ. Particle-imaging techniques for experimental fluid-mechanics. *Annu Rev Fluid Mech* 1991;23:261–304.
21. Keane RD, Adrian RJ. Theory of cross-correlation analysis of piv images. *Appl Sci Res* 1992;49:191–215.
22. Kaufmann TAS, Hormes M, Laumen M, et al. Flow distribution during cardiopulmonary bypass in dependency on the outflow cannula positioning. *Artif Organs* 2009;33:988–92.
23. Bellapart J, Geng S, Dunster K, et al. Intraaortic balloon pump counterpulsation and cerebral autoregulation: an observational study. *BMC Anesthesiol* 2010;10:3.
24. Hitosugi M, Niwa M, Takatsu A. Changes in blood viscosity by heparin and argatroban. *Thromb Res* 2001;104:371–4.